Chinese Chemical Letters 34 (2023) 108078

Contents lists available at ScienceDirect

Chinese Chemical Letters

journal homepage: www.elsevier.com/locate/cclet

# Fluorene pendant-functionalization of poly(*N*-vinylcarbazole) as deep-blue fluorescent and host materials for polymer light-emitting diodes

Ning Sun[a,b,1], Qin Zou[a,1], Wenyu Chen[a,1], Yingying Zheng[a], Kai Sun[a], Chunbin Li[b], Yamin Han[a], Lubing Bai[a], Chuanxin Wei[c], Jinyi Lin[a,*], Chengrong Yin[a,*], Jianguo Wang[b], Wei Huang[a,c,d,*]

[a] Key Laboratory of Flexible Electronics (KLOFE) and Institute of Advanced Materials (IAM), Nanjing Tech University (NanjingTech), Nanjing 211816, China
[b] College of Chemistry and Chemical Engineering, Inner Mongolia Key Laboratory of Fine Organic Synthesis, Inner Mongolia University, Hohhot 010021, China
[c] Centre for Molecular Systems and Organic Devices (CMSOD), Key Laboratory for Organic Electronics and Information Displays and Institute of Advanced Materials (IAM), Nanjing University of Posts and Telecommunications, Nanjing 210023, China
[d] Shaanxi Institute of Flexible Electronics (SIFE), Northwestern Polytechnical University (NPU), Xi'an 710072, China

ARTICLE INFO

*Article history:*
Received 16 October 2022
Revised 19 November 2022
Accepted 14 December 2022
Available online 17 December 2022

*Keywords:*
Poly(*N*-vinylcarbazole)
Fluorene
Deep-blue emission
Energy transfer
Polymer light-emitting diodes

ABSTRACT

$\pi$-Electron coupling of pendant conjugated segment in $\pi$-stacked semiconducting polymers always causes the formation of defect trapped sites and further quenched high-band excitons, which is harmful to the performance and stability of deep-blue polymer light-emitting diodes (PLEDs). Herein, considerate of "defect" carbazole (Cz) electromers in poly(N-vinylcarbazole) (PVK), a series of fluorene units are introduced into pendant segments (PVCz-DMeF, PVCz-FMeNPh and PVCz-DFMeNPh) to suppress the strong $\pi$-electron coupling of pendant Cz units and enhance radiative transition toward fabricating sable PLEDs. Compared to PVCz-FMeNPh and PVCz-DFMeNPh, PVCz-DMeF spin-coated films show a relatively efficient deep-blue emission, completely similar to its single pendant chromophore, confirmed an extremely weak charge-transfer and electron coupling between adjacent pendant segments. Therefore, PLEDs based on PVCz-DMeF present stable and deep-blue emission with a high color purity (0.17, 0.08), associated with extremely weak defect emission at 600~700 nm (induced by carbazole electromers). Finally, PLEDs based on PVCz-DMeF/F8BT blended films (1:1) also present the high maximum luminance ($L_{max}$) of 6261 cd/m$^2$ and current efficiency ($CE_{max}$) of 2.03 cd/A, confirmed slightly trapped sites formation. Therefore, precisely control the arrangement and packing model of pendant units in $\pi$-stacked polymer is an essential prerequisite for building efficient and stable emitter for optoelectronic devices.



In the last decades, semiconducting polymeric materials (SPMs) draw a great deal of attentions in fundamental research and industrial area, associated with their high performance, potential mechanical flexibility, low-cost solution processibility and easily structural modification, which are suitable for the preparation of organic optoelectronic devices, for instance organic light-emitting diodes (OLEDs) [1–4], organic field effect transistors (OFETs) [5–7], organic solar cells (OSCs) [8–10], organic thermoelectricity [11–14]. Up to date, according to the variable charge-transport channel, SPMs can be divided into two types: $\pi$-conjugated polymers and $\pi$-stacked polymers, that the former ones are associated with the oriented $\pi$-conjugated delocalization along backbone structure and the latter involved the $\pi$-electron coupling induced by the pendant conjugated units [1,15–20]. Compared to $\pi$-conjugated ones [21], the diversely topological structure of $\pi$-stacked polymers provide a platform to enhance and improve their performance and stability *via* controlling the hierarchically self-assembled structure, tuning the electron coupling between pendant units and regulating the chain conformation and phase [15,19,20,22–24]. Poly(*N*-vinylcarbazole) (PVK) as emblematic $\pi$-stacked polymers that present a series of advantages, such as excellent charge-transport mobility, outstanding charge capacity and multi-conformational behavior, which are widely used as host materials, hole

* Corresponding authors at: Key Laboratory of Flexible Electronics (KLOFE) and Institute of Advanced Materials (IAM), Nanjing Tech University (NanjingTech), Nanjing 211816, China.
*E-mail addresses:* iamjylin@njtech.edu.cn (J. Lin), iamcryin@njtech.edu.cn (C. Yin), wei-huang@njtech.edu.cn (W. Huang).
[1] These authors contributed equally to this work.

https://doi.org/10.1016/j.cclet.2022.108078
1001-8417/

transporting materials and multi-functional materials in OLEDs, OFETs and organic memory [1,15,20,25–27]. However, in fact, uncontrollable strong $\pi$-stacking behavior induced by the pendant carbazole units also results into the complicated photophysical processing, such as undesirable green-band emission, complex energy level and excitons-excitons annihilation, which are harmful to the performance and stability of optoelectronic devices [28–32]. What is more, the defect trapped sites caused by the strong carbazole stacking can quench the excitons, result into the low device performance and stability [28,29,33]. Therefore, precisely control the conformational behavior of pendant carbazole is a feasible strategy to enhance and stabilize the photophysical property of PVK-type $\pi$-stacked polymers toward fabricating the light-emitting optoelectronic devices.

In general, modular production enables organic conjugated materials to easily realize structural modification and precisely tune their photoelectrical and chem-physical property [34,35]. As an important conjugated segment, fluorene is an effective steric and aromatic $\pi$-conjugated segment to improve emission efficiency, tune energy level and enhance morphological stability, which are widely used to construct the novel high performance and stable conjugated materials [24,35–37]. To some context, introducing the fluorene into the carbazole of PVK polymers may suppress the $\pi$-stacking interaction and electron coupling of pendant conjugated group to enhance high emission efficiency, improve solution processing ability to strengthen film morphological stability and inhibit the formation of carbazole electromers "trap states" [1,24,34,36,37]. Then, in this work, considerate of $\pi$-conjugated and $\pi$-stacked transport channel, two design strategies are selected to obtain pendant fluorene-carbazole segment: directly conjugated bond to prolong conjugated effective length (Scheme 1, Type I), and $\pi$-conjugation-interrupted strategy to induce space-induce charge transfer (Scheme 1, Type II). Therefore, two-type $\pi$-stacked PVK polymers are prepared toward stable PLEDs: PVCz-DMeF (Type I) and PVCz-FMeNPh and PVCz-DFMeNPh (Type II). Firstly, all three polymers present excellent morphological stability and solution processing film-forming ability. More interestingly, corresponding spin-coated films showed a deep-blue emission that significantly different to parent PVK, attributed to the relatively weak $\pi$-stacking interaction of pendant fluorophore. Meanwhile, compared to the type II polymers, PVCz-DMeF-based PLEDs exhibited a stable deep-blue emission (CIE of (0.17, 0.08)) and a better device performance, associated with the completely suppression of trapped sites. Finally, due to excellent Förster resonance energy transfer (FRET) and low trapped sites, PLEDs based on PVCz-DMeF/poly(9,9-dioctylfluorene-co-benzothiadiazole) (F8BT) blended layer exhibited better performances than those of device based on purify F8BT, PVK/F8BT films, confirming the availability of our strategy and with a wide range of potential for optoelectronics applications in the future.

**Table 1**
Fundamental and Structural property of three polymers.

| Polymer | $M_n$ (kDa) | PDI | $T_d$ (°C) | $T_g$ (°C) | HOMO, LUMO (eV) | $S_1$ (eV)[a] |
|---|---|---|---|---|---|---|
| PVCz-DMeF | 40.8 | 1.88 | 449 | 244 | −5.50, −2.65 | 3.22 |
| PVCz-FMeNPh | 13.4 | 1.30 | 393 | 193 | −5.01, −2.56 | 2.81 |
| PVCz-DFMeNPh | 17.8 | 1.35 | 441 | 208 | −4.92, −2.60 | 2.73 |

[a] It is calculated from low temperature PL spectra.

PVCz-DMeF, PVCz-FMeNPh and PVCz-DFMeNPh, in which the fluorene group is modified on either side or both sides of the carbazole core, are prepared *via* radical polymerization (Scheme 1c) [36,38]. The chemical structures of the three monomers were verified *via* NMR spectral measurement, as shown in Fig. S1 (Supporting information). The polydispersity index (PDI) and number average molecular weight ($M_n$) are 1.88 and 40.8 kDa for PVCz-DMeF, 1.30 and 13.5 kDa for PVCz-FMeNPh, 1.35 and 17.8 kDa for PVCz-DFMeNPh (Table 1), respectively, that monitored by gel permeation chromatography (GPC) (Fig. S2 in Supporting information). According to the thermogravimetric analysis (TGA) results, three polymers have high decomposition temperatures ($T_d$), which are about 449 °C, 393 °C and 441 °C for PVCz-DMeF, PVCz-FMeNPh and PVCz-DFMeNPh, respectively (Fig. S3 in Supporting information). Then, differential scanning calorimetry (DSC) characterization of PVCz-DMeF, PVCz-FMeNPh and PVCz-DFMeNPh showed glass transition temperatures ($T_g$) to be 244 °C, 193 °C and 208 °C, respectively (Fig. S3). Meanwhile, all three polymers had well solubility in common organic solvents, such as toluene and $CHCl_3$, which is useful to obtain smooth spin-coated film *via* solution processing technology.

In general, photophysics property are frequently-used measurement to probe the chain arrangement and aggregation behavior [15,39]. Therefore, UV–vis absorption and fluorescence spectra of PVCz-DMeF, PVCz-FMeNPh and PVCz-DFMeNPh in various states were obtained to elucidate their photophysical properties, as shown in Fig. 1. The maximum absorption peak of the PVCz-DMeF pristine spin-coated film is estimated about 319 nm, and the maximum emission peak are at 403 nm. Besides, similar PL spectral profiles of annealed films were obtained under thermal treatment at 180 °C and 200 °C also revealed excellent deep-blue emission stability (Fig. 1a and Fig. S4 in Supporting information). Notablely, the absorption and emission spectra of PVCz-DMeF in the dilute

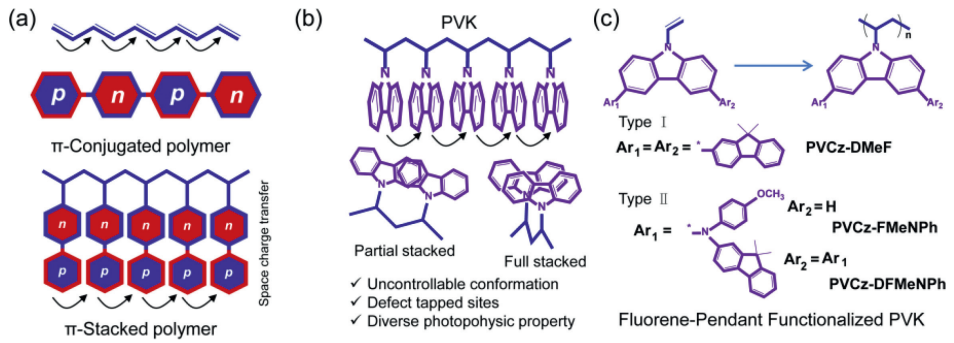


**Scheme 1.** Molecular design principle of model fluorene pendant-functionalized $\pi$-stacked PVK. (a) Two types of typical semiconducting polymeric materials (SPMs): $\pi$-conjugated polymers and $\pi$-stacked polymers. (b) Chemical structure of PVK. Two-types $\pi$-stacked conformation of pendant carbazoles (Cz) in PVK are observed to induce the formation of "trap states" carbazole electromers: full stacked and partial stacked ones, which may result into an uncontrollable conformational behavior, undesirable defect "trapped sites" and diverse photophysical property in solid states. (c) Schematic representation of the isolated pendant group in fluorene-functionalized PVK. Compared to the parent $\pi$-stacked Cz units in PVK chain, pendant fluorene-Cz groups may present excellent film forming ability with a stable morphology, weakly direct stacking interaction between adjacent Cz units, suppress the defect formation toward fabricating light-emitting devices.

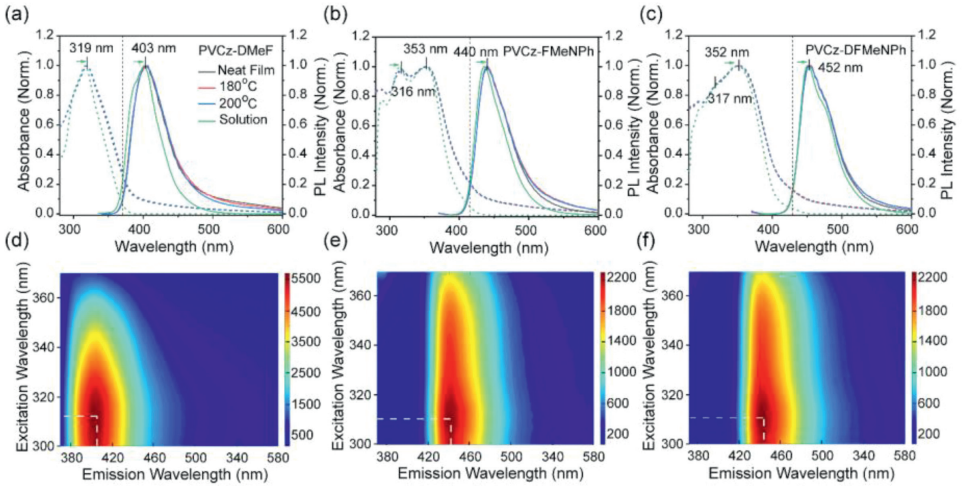


**Fig. 1.** Optical property of three polymers in various states. Steady absorption (dotted line) and PL (solid line) spectra of (a) PVCz-DMeF, (b) PVCz-FMeNPh and (c) PVCz-DFMeNPh in diluted toluene solution, pristine film and annealed films (180 °C or 200 °C thermal annealed for 10 min). 3D PL mapping spectra of (d) PVCz-DMeF, (e) PVCz-FMeNPh and (f) PVCz-DFMeNPh for pristine films.

solution are similar to those in film state, indicated single pendant fluorophore emission behavior [40]. Moreover, the full-width-half-maximum (FWHM) of PVCz-DMeF in the solution and pristine film are estimated about 50 nm and 56 nm, also confirmed narrow-band deep-blue emission [41]. Similarly, the same absorption and PL spectral profile between dilute solution and film state are found for the PVCz-FMeNPh and PVCz-DFMeNPh, also indicate the similar excitonic behavior. The maximum absorption and emission peaks of PVCz-FMeNPh and PVCz-DFMeNPh pristine films are located at 353 nm and 440 nm (Fig. 1b), 352 nm and 452 nm (Fig. 1c), respectively. Compared to the PVCz-DMeF, both these peaks at relatively long-wavelength effectively confirmed the relatively strong charge-transfer between adjacent pendant Cz units, TPA and fluorene units in PVCz-FMeNPh and PVCz-DFMeNPh. Corresponding FWHM of the pristine films are 54 nm and 54 nm, respectively. Both two materials spin-coated films had stable blue emission without any obvious green-band emission after thermal annealing (Fig. 1 and Fig. S4). Besides, 3D PL mapping spectrograms reveal that all three polymers present one emissive sites with a stable deep-blue emission (Figs. 1e and f, Fig. S5 in Supporting information). Meanwhile, the life-times of all three-type spin-coated films at blue-band emission are calculated about 1–2 ns, respectively, and corresponding PLQY are estimated about 12.7%, 3.5% and 3.6% (Fig. S6 and Table S1 in Supporting information). Besides, compared to the PVCz-FMeNPh and PVCz-DFMeNPh ones, the PVCz-DMeF pristine and annealed films have relatively high radiative transition rate, which is more beneficial to fabricate light emitting devices. In general, PVCz-DMeF, PVCz-FMeNPh and PVCz-DFMeNPh have similar flexible polyethylene backbone and carbazole core. Directly linked between fluorene and carbazoles in PVCz-DMeF may prolong the effective conjugated length to enhance the emission efficiency, but serious charge-transfer and electron coupling between fluorene, TPA and carbazoles observed for PVCz-FMeNPh and PVCz-DFMeNPh [19,20], which result into distinct photophysical properties. Compared to parent PVK materials, the similarity of the PL spectra of the three polymers solution state and spin-coated films revealed the synergistic effect between the main and side chain luminescence elements of flexible polyethylene, which can effectively avoid chromophore aggregation, reduce the adverse effects caused by exciton coupling, and improve its photoelectric properties.

Besides, cyclic voltammetry (CV) analysis revealed that the highest occupied molecular orbital (HOMO) level is lifted up upon incorporation *N*-(4-methoxyphenyl)−9,9-dimethyl-9*H*-fluoren-2-amine (FMeNPh) unit, thus causing a relatively narrow bandgap and redshifted optical spectra, consistent with the results of the density functional theory (DFT) (Figs. S7 and S8 in Supporting information, Table 1). Meanwhile, the distribution of electron clouds for HOMO and LUMO are obtained upon optimizing the geometric configuration (Fig. S7). And that of the PVCz-DMeF chromophore basically coincide, revealing that electrons are distributed on the whole chromophore, indicating that the chromophore is conjugated structure on which electrons are in delocalized state (Fig. S7a). The HOMO orbital of the PVCz-FMeNPh and PVCz-DFMeNPh are mostly distributed on the carbazole core, and partly distributed on the fluorene group of FMeNPh unit, indicating that their conjugation degree is not as high as that of PVCz-DMeF. The electron cloud on the LUMO orbital is mainly distributed on the carbazole segment reveals that carbazole is an electron-withdrawing group in the system (Figs. S7b and c). The quantum efficiency (PLQY) of PVCz-DMeF, PVCz-FMeNPh and PVCz-DFMeNPh are lower with smaller radiative transition rate ($k_r$), and the non-radiative transition rate ($k_{nr}$) is at least 7 times higher than $k_r$. Therefore, PVCz-DMef, PVCz-FMeNPh and PVCz-DFMeNPh may be used as the host materials in PLEDs.

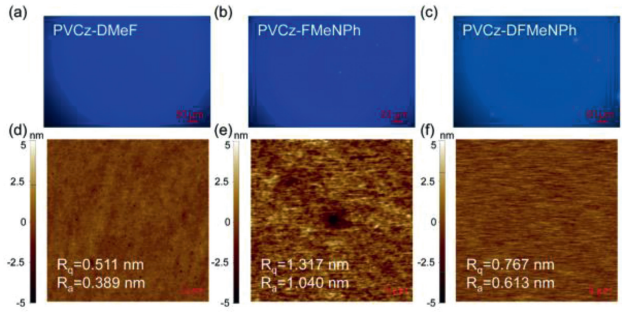


**Fig. 2.** Morphological property of three polymers in film states. Fluorescence microscope (FLM) images of (a) PVCz-DMeF, (b) PVCz-FMeNPh and (c) PVCz-DFMeNPh pristine films, together with (d-f) their corresponding AFM images.

Notablely, the morphology of thin film affects the performance of light-emitting devices. Subsequently, we also carried out fluorescence microscope (FLM) and atomic force microscopy (AFM) to monitor the emission behavior and morphological stability of three polymers spin-coated films (Fig. 2). For PVCz-DMeF material,

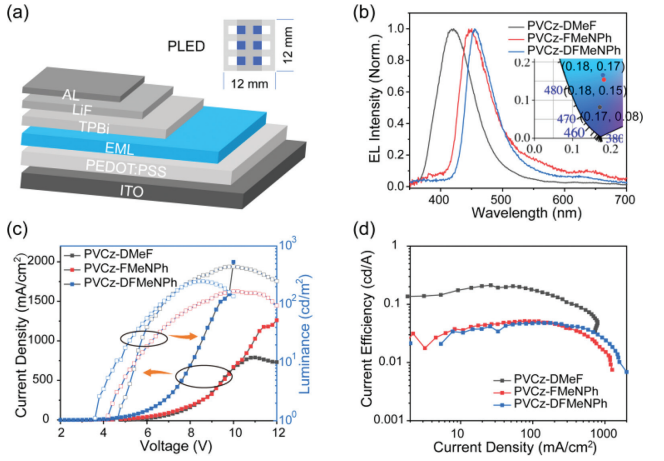


**Fig. 3.** Blue PLEDs based on the three PVK type polymers. (a) Diagram of the PLED (ITO/PEDOT:PSS/EML/TPBi/LiF/Al). (b) Electroluminescence (EL) spectra of PVCz-DMeF, PVCz-FMeNPh and PVCz-DFMeNPh. The inset shows the CIE coordinate diagram at 9 V. Corresponding current densities are about 1500 mA/cm$^2$, 400 mA/cm$^2$ and 405 mA/cm$^2$. (c) Current density & luminance *versus* voltage characteristics and (d) current efficiency *versus* current density curves for devices based on PVCz-DMeF, PVCz-FMeNPh and PVCz-DFMeNPh, respectively.

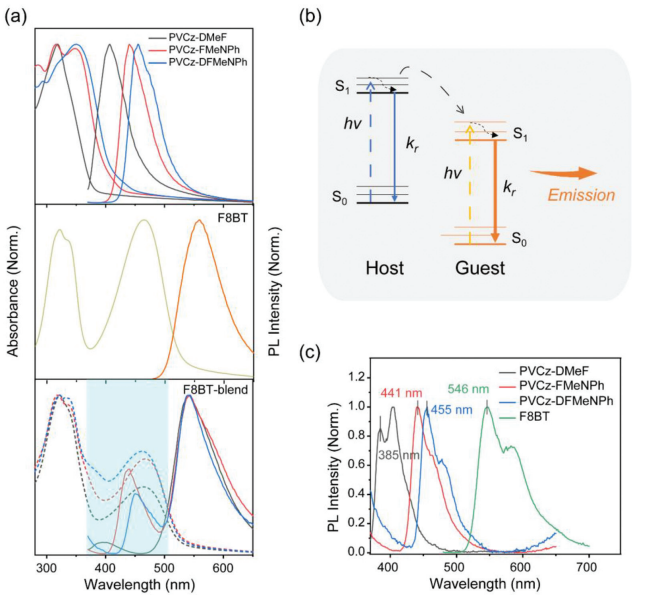


**Fig. 4.** Energy transfer from host PVK-type polymers to F8BT in film states. (a) Normalized absorption and PL spectra of three polymers films (top, PVCz-DMeF, PVCz-FMeNPh and PVCz-DFMeNPh), F8BT film (middle) and three polymers blended with F8BT films (bottom, PVCz-DMeF/F8BT for black line, PVCz-FMeNPh/F8BT for red line and PVCz-DFMeNPh for blue line). (b) Energy level schematic for host PVK-type polymers and guest F8BT. The corresponding vertical absorption values are approximated by theoretical calculations. (c) Low temperature fluorescence spectra of PVCz-DMeF, PVCz-FMeNPh, PVCz-DFMeNPh and F8BT films.

pristine film presents smooth and continuous state, indicated their excellent film formation ability and deep-blue emission (Fig. 2a). In contrast, the solubility and film-forming ability of PVCz-FMeNPh and PVCz-DFMeNPh were slightly inferior, and the luminescence of PVCz-DFMeNPh shows a relatively weak deep-blue emission under the fluorescence microscope (Figs. 2b and c). The results of AFM also show that three polymers are smooth and uniform for pristine films with low root mean square roughness (RMS) of 1.314, 1.266 and 1.251 nm (Figs. 2d–f), respectively, consistent with the fluorescence microscopy results above. The good film forming ability and uniform film morphology of the three materials are conducive to the solution preparation process of the device.

Subsequently, the polymer light-emitting diodes (PLEDs) were fabricated with the configuration structure of ITO/PEDOT:PSS/EML/TPBi/LiF/Al to investigate their electroluminescene (EL) properties (Fig. 3a). PVCz-DMeF, PVCz-FMeNPh and PVCz-DFMeNPh films are introduced to as the emission layers for the PLEDs. Figs. 3b–d show the performance of PLED based on PVCz-DMeF, PVCz-FMeNPh and PVCz-DFMeNPh. As we expected, EL spectra of device based on PVCz-DMeF show a maximum peak at 419 nm with a FWHM of 69 nm, similar to the PL spectral profiles, indicate a weak energy transfer under applied electrical field. And corresponding CIE is about (0.17, 0.08), also confirmed its excellent deep-blue emission (Fig. 3b, Figs. S10 and S11, Table S2 in Supporting information). More interestingly, compared to the serious carbazole electromers in PVK, no obvious emission at 600∼700 nm is observed for the PVCz-DMeF-based PLEDs. Therefore, directly link between the fluorene and carbazole in PVCz-DMeF can effectively suppress the $\pi$-$\pi$ stacking interaction of carbazole in PVK and avoid the formation of trapped sites in solid states. Similarly, emission peaks are estimated about at 450 nm and 455 nm, for PVCz-FMeNPh and PVCz-DFMeNPh-based PLEDs. Corresponding CIE are about (0.18, 0.15) and (0.18, 0.17), respectively, indicated a sky-blue emission. However, there is a weak emission band at 600-650 nm found in corresponding EL spectra, indicated a weak carbazole electromers or excimer emission induced by the pendant chromophore (Fig. 3b) [28,29]. And these emission bands at long-wavelength are enhanced with increasing applied voltage, also confirmed the weak energy transfers. Then, $\pi$-conjugation-interrupted strategy in this pendant-functionalization may result into forming residual carbazole electromers and strong energy transfer. Of course, it needs to note that there is weak emission at long-wavelength observed under high current density (1000 mA/cm$^2$) in all PLEDs. Therefore, PVCz-DMeF-based device exhibited the maximum luminance ($L_{max}$) of 442 cd/m$^2$ with the $V_{on}$ of 4.7 V, the current efficiency (*CE*) of 0.21 cd/A and the EQE of 0.44%, whereas the PVCz-FMeNPh and PVCz-DFMeNPh-based present the $L_{max}$ of 166 cd/m$^2$, 246 cd/m$^2$ with the $V_{on}$ of 4.2 V, 3.6 V, the *CE* of 0.05 cd/A, 0.05 cd/A and the EQE of 0.04%, 0.04%, respectively (Fig. S9 and Table S2 in Supporting information). In this regard, compared to other two polymers, PVCz-DMeF-based PLEDs had a better stable color purity of deep-blue emission, current efficiency, brightness and low $V_{on}$, which may also potential candidate as host materials for PLEDs.

To further explore the existence of energy transfer between the three materials and F8BT in doping system, we further monitored the absorption and emission spectra of the three materials, F8BT and their blends (Fig. 4a and Fig. S12 in Supporting information). PL spectra of PVCz-DMeF, PVCz-FMeNPh and PVCz-DFMeNPh have been described above. The absorption spectra of F8BT with a maximum peak at 465 nm partially overlaps with the emission spectra of PVCz-DMeF, and almost completely covers the emission spectral range of PVCz-FMeNPh, PVCz-DFMeNPh, proves that efficient FRET energy transfer from host (novel polymers) to guest (F8BT) can be observed in the doping system. Under the doping ratio of 1:1 between host and guest materials, emission peaks at short-wavelength belonging to the host materials are appeared, suggested the incomplete energy transfer. In general, compared to the photo-excitation, relatively strong energy transfer may occur under electrical field. Therefore, we set the doping ratio of 1:1 between PVCz-DMeF, PVCz-FMeNPh, PVCz-DFMeNPh and F8BT to systematically investigate the energy transfer and their application in PLEDs. Taking the monomer chromophor of the host and guest material as the unit, the vertical absorption of the material was approximately calculated by DFT, and the values of materials $S_1$ were 3.67 eV,

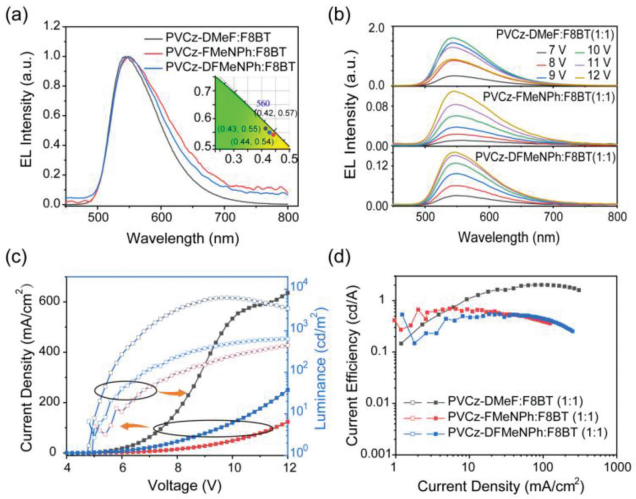


**Fig. 5.** PLEDs based on the PVCz-DMeF/F8BT, PVCz-FMeNPh/F8BT and PVCz-DFMeNPh/F8BT films with the doping ratio of 1:1. (a) EL spectra of corresponding devices at 9 V. The inset shows the corresponding CIE color coordinate diagram at 9 V. (b) EL spectra of corresponding devices at various voltages. (c) Current density & luminance *versus* voltage characteristics and (d) current efficiency *versus* current density curves for corresponding devices.

3.09 eV, 2.93 eV and 2.84 eV, respectively. As shown in Fig. 4b, there is the possibility of energy transfer between host and guest, and the low-temperature fluorescence measurements also support this assumption (Fig. 4c).

Therefore, preliminary PLEDs were fabricated with conventional configuration of ITO/PEDOT:PSS/EML/ TPBi/LiF/Al to check the energy transfer from PVK-type polymer to F8BT. Emissive layers are obtained using the doped 1:1 ratio of PVK type polymers (host) and F8BT (guest). Corresponding device performances are shown in Fig. 5. As we expect, all PLEDs present a maximum peak at 543 nm without any deep-blue emission at high-band, indicated a completely energy transfer from PVK type polymers to F8BT under electrical field. And corresponding CIE are about (0.42, 0.57), (0.44, 0.54) and (0.43, 0.55). However, as we discussed above, the residual trapped sites were existed in PVCz-FMeNPh, PVCz-DFMeNPh, and further quenched exciton from F8BT in PLEDs, which may reasonably result into low device performance and stability [28,29]. Therefore, as shown in Fig. 5c, it is clearly found that PLEDs based PVCz-DMeF/F8BT present better current efficiency, brightness than those of PVCz-FMeNPh/F8BT, PVCz-DFMeNPh/F8BT ones. In details, PLEDs based on PVCz-DMeF/F8BT blended films displayed $V_{on}$ of 4.7 V, the $L_{max}$ of the 6261 cd/m$^2$, with $CE_{max}$ is 2.03 cd/A, respectively, which are comparable to conventional blended F8BT devices but higher than those of device based on purified F8BT films [42]. The value of $V_{on}$, $L_{max}$ and $CE_{max}$ for PVCz-FMeNPh/F8BT and PVCz-DFMeNPh/F8BT based devices are estimated about 5.0 V, 445 cd/m$^2$, 0.70 cd/A and 4.8 V, 636 cd/m$^2$, 0.54 cd/A, respectively (Fig. S13 and Table S2 in Supporting information). Meanwhile, PVCz-DMeF/F8BT based doped device present more stable emission spectra, located in the yellow-green region (Fig. S14 in Supporting information). Therefore, PLED based on PVCz-DMeF/F8BT have better device performance than other devices of the same type, associated with the suppression of the formation of trapped sites, consistent with the previous analysis.

In summary, we demonstrated a simple pendant-functionalized strategy to suppress the formation of carbazole electromers in $\pi$-stacked PVK materials *via* introducing the steric fluorene unit into the pendant conjugated units. Different to the $\pi$-conjugation-interrupted linked fluorene units in PVCz-FMeNPh and PVCz-DFMeNPh, PVCz-DMeF spin-coated films present a robust single pendant-chromophore emission behavior at 419 nm without obvious narrow-band long-wavelength emission, which may induce by the strong $\pi$-electron coupling and space charge-transfer of pendant carbazole segment. These carbazole electromers are observed in the EL spectra of PVCz-FMeNPh and PVCz-DFMeNPh-based PLEDs, which are trapped high-band excitons and reduced device performance. As we expected, PVCz-DMeF-based PLEDs had an excellent deep-blue emission with CIE of (0.17, 0.08), associated with the single-chromophore photophysical processing. More interestingly, PLEDs based on PVCz-DMeF/F8BT blended films show better current efficiency (2.05 cd/A, >3 folds) and higher maximum brightness (6261 cd/m$^2$, > 10 folds) than those of controlled ones, also confirmed the weak exciton quenching by defect trapped sites in solid states. Therefore, the pendant steric functionalization of $\pi$-stacked semiconducting polymers is an effective strategy to precisely control their excitonic behavior and photophysical processing toward the optoelectronic devices.

## Declaration of competing interest

The authors declare no conflict of interest.

## Acknowledgments

The work was supported by the National Natural Science Foundation of China (Nos. 22105099 and 61874053), and Natural Science Foundation of Jiangsu Province (No. BK20200700), the China Postdoctoral Science Foundation (No. 2022M711591), the open research fund from Anhui Province Key Laboratory of Optoelectronic Materials Science and Technology (No. OMST202101), the State Key Laboratory of Luminescent Materials and Devices (South China University of Technology).

## Supplementary materials

Supplementary material associated with this article can be found, in the online version, at doi:10.1016/j.cclet.2022.108078.

## References

[1] J.Y. Lin, B. Liu, M.N. Yu, et al., Adv. Mater. 31 (2019) 1804811.
[2] D.H. Kim, A. D'Aléo, X.K. Chen, et al., Nature Photon 12 (2018) 98–104.
[3] T. Higuchi, H. Nakanotani, C. Adachi, Adv. Mater. 27 (2015) 2019–2023.
[4] L.J. Tu, Y.J. Xie, Z. Li, B.Z. Tang, SmartMat 2 (2021) 326–346.
[5] Y. Zheng, G.J.N. Wang, J. Kang, M. Nikolka, et al., Adv. Mater. 29 (2019) 11905340.
[6] J. Mun, J. Kang, Y. Zheng, et al., Adv. Mater. 31 (2019) 1903912.
[7] Y. Kim, S. Chung, K. Cho, et al., Adv. Mater. 31 (2019) 1806697.
[8] Z.T. Rong, X.Z. Guo, S.S. Lian, et al., Adv. Funct. Mater. 29 (2019) 1904018.
[9] B.L. Li, K. Yang, Q.G. Liao, et al., Adv. Funct. Mater. 31 (2021) 2100332.
[10] R. Cao, Y. Chen, F.F. Cai, et al., J. Cent. South Univ. 27 (2020) 3581–3593.
[11] Y. Lu, J.Y. Wang, J. Pei, Chem. Mater. 31 (2019) 6412–6423.
[12] J. Guo, G.D. Li, H. Reith, et al., Adv. Electron. Mater. 6 (2020) 1900945.
[13] P. Baronas, G. Kreiza, M. Mamada, et al., Adv. Opt. Mater. 8 (2020) 1901670.
[14] X.B. Yu, C. Li, C.Y. Gao, et al., SmartMat 2 (2021) 347–366.
[15] L.H. Xie, Q.D. Ling, X.Y. Hou, W. Huang, J. Am. Chem. Soc. 130 (2008) 2120–2121.
[16] A.J. Heeger, Chem. Soc. Rev. 39 (2010) 2354–2371.
[17] J.Y. Ouyang, SmartMat 2 (2021) 263–285.
[18] K. Zhou, K. Dai, C. Liu, et al., SmartMat 1 (2020) e1010.
[19] J. Hu, Q. Li, X.D. Wang, et al., Angew. Chem. Int. Ed. 58 (2019) 8405–8409.
[20] S.Y. Shao, J. Hu, X.D. Wang, et al., J. Am. Chem. Soc. 139 (2017) 17739–17742.
[21] B.G. Kim, E.J. Jeong, J.W. Chung, et al., Nat. Mater. 12 (2013) 659–664.
[22] L.Y. Wang, H.Y. Tsai, H.C. Lin, Macromolecules 43 (2010) 1277–1288.
[23] T.C. Liang, H.C. Lin, J. Polym. Sci. Part A: Polym. Chem. 47 (2009) 2734–2753.
[24] L. Li, T.Q. Hu, C.R. Yin, et al., Polym. Chem. 6 (2015) 983–988.
[25] M. Cai, T. Xiao, Y. Chen, et al., Appl. Phys. Lett. 99 (2011) 254.
[26] P.L. Gao, J.N. Wang, L.H. Wang, et al., Org. Electron. 92 (2021) 106138.
[27] P. Wang, C.P. Chai, F.Z. Wang, et al., J. Polym. Sci. Part A: Polym. Chem. 46 (2008) 1843–1851.
[28] V. Jankus, A.P. Monkman, Adv. Funct. Mater. 21 (2011) 3350–3356.
[29] T.L. Ye, J.S. Chen, D.G. Ma, Phys. Chem. Chem. Phys. 12 (2010) 15410–15413.
[30] L. Qian, D. Bera, P.H. Holloway, Appl. Phys. Lett. 92 (2008) 053303.
[31] B. Hu, Z. Yang, F.E. Karasz, J. Appl. Phys. 76 (1994) 2419–2422.

[32] X.J. Xu, G. Yu, C. Di, Y.Q. Liu, Appl. Phys. Lett. 89 (2006) 123503.
[33] J.Y. Li, D. Liu, C.W. Ma, et al., Adv. Mater. 16 (2004) 1538–1541.
[34] L.H. Xie, C.R. Yin, W.Y. Lai, W.Y. Lai, W. Huang, Prog. Polym. Sci. 37 (2012) 1192–1264.
[35] X. An, J.H. Yang, M. Xu, et al., Chin. Chem. Lett. 33 (2022) 5137–5141.
[36] Y.M. Han, L.B. Bai, J.Y. Lin, et al., Adv. Funct. Mater. 31 (2021) 2105092.
[37] N. Sun, Y.M. Han, L.L. Sun, et al., Macromolecules 54 (2021) 6525–6533.
[38] Z.W. Pan, H. Gao, Y.Y. Yang, et al., J. Energy Chem. 69 (2022) 123–131.
[39] K. Matti, A.P. Monkman, Adv. Mater. 25 (2013) 1090–1108.
[40] F. Cacialli, J.S. Wilson, J.J. Michels, et al., Nat. Mater. 1 (2002) 160–164.
[41] B. Cao, M.H. Hu, Y. Cheng, et al., NPG Asia Mater. 13 (2021) 1–36.
[42] L.B. Bai, C. Sun, Y.M. Han, et al., Adv. Opt. Mater. 8 (2020) 1901616.